Chemical Papers (2018) 72:1619–1628
https://doi.org/10.1007/s11696-017-0374-6

ORIGINAL PAPER

Reduction of silver ions to silver with polyaniline/poly(vinyl alcohol) cryogels and aerogels

Patrycja Bober[1] · Miroslava Trchová[1] · Jana Kovářová[1] · Udit Acharya[1,2] · Jiřina Hromádková[1] · Jaroslav Stejskal[1]

Received: 3 November 2017 / Accepted: 21 December 2017 / Published online: 24 January 2018

Abstract
The macroporous conducting polymer cryogels were prepared by the oxidation of aniline hydrochloride in the frozen aqueous solutions of poly(vinyl alcohol) at − 24 °C. Corresponding polyaniline aerogels supported with poly(vinyl alcohol) have been obtained after thawing of cryogels followed by freeze-drying. Silver was deposited on the composites using the ability of polyaniline to reduce silver ions after the immersion in silver nitrate solutions. Swollen cryogels were coated only on the surface with macroscopic silver particles due to the closed-pore structure in cryogels and limited penetration of silver ions into macropores. The diffusion of silver ions to freeze-dried aerogels was better and further improved by vacuum treatment. Silver microcubes were produced in the pores, the weight fraction of silver in dry composites being typically several per cent, a maximum 13 wt%. The conductivity of the aerogels compressed to pellets depended on the processing and the highest value was 0.27 S cm^{-1}. The aerogels containing silver were characterized in detail with Raman spectroscopy.

Keywords Conducting polymer · Polyaniline · Cryogel · Aerogel · Silver · Silver microcubes

Introduction

The composites of conducting polymers, such as polyaniline (Stejskal et al. 2010), and noble metals have often been reported in the literature as the way to combine the organic semiconductors and metals (Han et al. 2017a). Among them, those with silver have been investigated most frequently (Stejskal 2013). Such composites failed to display the expected high conductivity, because metal nanoparticles could not produce the efficient conducting pathways at reasonably low metal contents. The special types of composites with the conductivity independent over a broad temperature range could be of some interest (Bober et al. 2011). In general, however, applications that do not require high conductivity are oriented to analytical detection and sensors (Wang et al. 2013; Rahman et al. 2016; Zhang et al. 2016; Pande et al. 2017; Pandey et al. 2017; Wang et al. 2017a; Xu et al. 2017), antibacterial compositions (Hou et al. 2016; Maráková et al. 2017; Salam et al. 2017; Zhao et al. 2017), electrocatalysts (Yi et al. 2014), photocatalysts (Wang et al. 2017b), and energy-conversion devices (Pan et al. 2016; Tang et al. 2016; ul Haque et al. 2017).

There are three ways how to prepare polyaniline/silver composites (Stejskal 2013; Bober et al. 2014): (1) by the mixing of both components (Khan et al. 2016; Xu et al. 2017); (2) by the oxidation of aniline with silver ions in aqueous medium (Wang et al. 2013; Ma et al. 2016; Saleh et al. 2016); and (3) by reduction of silver ions with polyaniline (Trchová and Stejskal 2010; Pan et al. 2016; Maráková et al. 2017). The composites were obtained as powders. For the specific applications, however, another component has been introduced to provide the utility properties, and carbon nanotubes (Tang et al. 2016; Salam et al. 2017), inorganic oxides (Pan et al. 2016), textiles (Maráková et al. 2017), or membranes (Zhao et al. 2017) might serve as examples.

Conducting hydrogels (Stejskal 2017) represent new class of conducting materials that have been recognized especially for their applications in biomedicine (Guiseppi-Elie 2010). The preparation of novel type, macroporous

This work was presented at the 81st Prague Meeting on Macromolecules held on September 10–14, 2017.

✉ Patrycja Bober
bober@imc.cas.cz

[1] Institute of Macromolecular Chemistry, Academy of Sciences of the Czech Republic, 162 06 Prague 6, Czech Republic

[2] Faculty of Mathematics and Physics, Charles University, 121 16 Prague 2, Czech Republic

polyaniline cryogels supported with poly(vinyl alcohol), has recently been emerged (Stejskal et al. 2017). Such composite material is tested as a support for the deposition of silver in the present communication.

Experimental

Preparation of polyaniline–poly(vinyl alcohol) cryogel and aerogel

Polyaniline/poly(vinyl alcohol) cryogels have been prepared by oxidation of 0.2 M aniline hydrochloride (Penta, Czech Republic) with 0.25 M ammonium peroxydisulfate (Lach-ner, Czech Republic) in 5 wt% aqueous solution of poly(vinyl alcohol) (PVAL; Mowiol 10–98, Sigma Aldrich; M_w = 61,000; 5 wt% PVAL = 1.14 M of PVAL constitutional units). Each reactant was dissolved separately in 5 wt% aqueous solution of poly(vinyl alcohol). Both solutions were mixed and the mixture was immediately sucked into a plastic syringe, quickly frozen in solid carbon dioxide/ethanol suspension, and then left in a freezer at − 24 °C for 5 days to polymerize. After polymerization took place, the syringes were removed from freezer and the content was left for 3 h to thaw at room temperature. The cryogels were then removed from the syringe, and immersed in excess of water for 2 weeks to remove any residual reactants and by-products. They contained ca 2 wt% polyaniline, 5 wt% PVAL, and 93 wt% water (Stejskal et al. 2017). The aerogels were prepared by freeze-drying of cryogels for 24 h in a CoolSafe Pro (Scanvac, Denmark). The aerogels were composed of ca 58 wt% polyaniline and 42 wt% of PVAL (Stejskal et al. 2017). The content of polyaniline may somewhat vary depending on the degree of protonation.

Reduction of silver ions by polyaniline

Silver ions are reduced by polyaniline to metallic silver (Fig. 1). The swollen cryogels or aerogels were immersed in silver nitrate solutions in 1 M methanesulfonic acid for 5 days at room temperature. In the case of aerogels, the samples immersed in the solution were either left at rest for 2 weeks or they were placed for 30 min into rotational evaporator and the air pressure was reduced to remove air from aerogels and to allow for faster penetration of silver nitrate solution inside. The resulting composite hydrogels were then transferred to water, and after exhaustive removal of residual silver nitrate and methanesulfonic acid, they were freeze-dried.

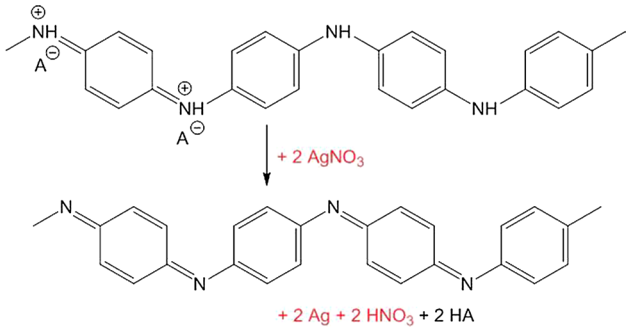

Fig. 1 Polyaniline salt in emeraldine oxidation state reduces silver nitrate to silver metal and at the same time becomes oxidized to pernigraniline. A^- is an arbitrary anion, here mainly methanesulfonate, $CH_3SO_3^-$

Characterization

Electron scanning micrographs have been taken using a JEOL 6400 microscope. The DC electrical conductivity was determined by van der Pauw method on pellets of a 13 mm diameter and 1 ± 0.2 mm thickness prepared with a manual hydraulic press Trystom H-62 at 70 kN. The silver content was determined as a residue in thermogravimetric analysis (TGA) performed in 50 cm^3 min^{-1} air flow at the heating rate of 10 °C min^{-1} to 800 °C with a Pyris 1 Thermogravimetric Analyzer (Perkin Elmer, USA).

Raman spectra were recorded with a Renishaw InVia Reflex Raman microspectrometer. The spectra were excited with argon-ion 514 nm and near-infrared diode 785 nm lasers. A research-grade Leica DM LM microscope with 50× objective magnification was used to focus the laser beam. The scattered light was analyzed with a spectrograph using holographic gratings 2400 and 1200 lines mm^{-1}, respectively. A Peltier-cooled charge-coupled detector (576 × 384 pixels) registered the dispersed light. The spectra were recorded with the highest power that still did not alter the sample by heating. Polyaniline aerogels were analyzed with a 514 nm laser excitation line or, pressed in pellets, with a 785 nm laser.

Results and discussion

Preparation of cryogels and aerogels

The preparation of polymer cryogels (Stejskal et al. 2017) is based on the polymerization of a suitable monomer, here aniline hydrochloride, in frozen reaction mixture, i.e., in ice (Konyushenko et al. 2008), in the presence of supporting water-soluble polymer. A typical reaction mixture thus contains a monomer, ammonium peroxydisulfate oxidant,

and poly(vinyl alcohol) dissolved in water. When the aniline oxidation proceeds in the liquid state at room temperature, submicrometre colloidal polyaniline dispersions stabilized with poly(vinyl alcohol) are produced (Stejskal et al. 1996; Wang et al. 2017c). When the same reaction was carried out in solid ice, the composite cryogel was produced instead (Stejskal et al. 2017). During the freezing, the generated ice crystals expel the solutes, which concentrate in the coexisting liquid phase between the crystals (Lozinsky and Okay 2014). The polymerization in the space between the crystals produces a gel framework. After thawing, the melted ice crystals are responsible for the macropores filled with water. Such scenario anticipates that the cryogels will have a predominating closed-pore structure. Cryogels can be prepared in any shape depending on reaction vessel, e.g., in polyethylene syringes (Fig. 2). After freeze-drying, the so-called aerogels are produced. They are macroporous with the pores sizes in tens of micrometre range (Fig. 3).

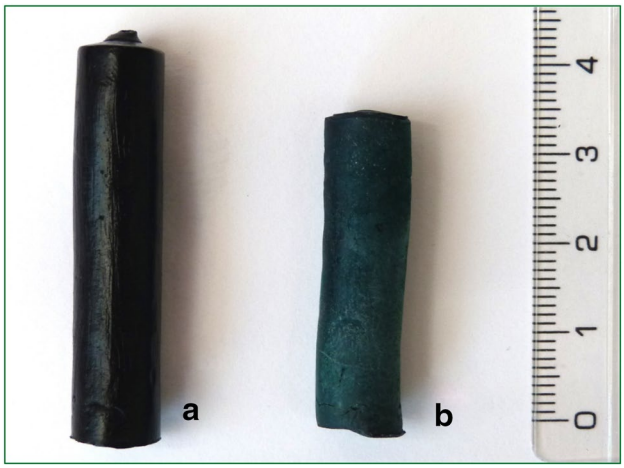

Fig. 2 **a** Swollen cryogel and **b** freeze-dried aerogel. The scale is in centimetres

Silver deposition on cryogels

Polyaniline in cryogels supported with poly(vinyl alcohol) has been used as a reductant of silver ions in 1 M methanesulfonic acid (Fig. 1). This acid was selected, because it does not precipitate silver ions unlike most of inorganic ones. Molar concentrations of silver nitrate have been varied from 0.001 to 0.1 M. The water-swollen cryogels obtained after preparation (Fig. 2) have been immersed in the silver nitrate solutions. Silver, however, was deposited in negligible amount only on the cryogel surface as particles tens of micrometres in size, which were identified at back-scattered electron images (Fig. 4). This reflects the fact that the cryogel is composed of closed macropores which do not allow for the efficient penetration of silver nitrate solution into the interior of cryogel.

Silver deposition on aerogels

For above reason, the air-dried cryogels, aerogels, have been used in subsequent experiments. It was expected that the freeze-drying would enhance the accessibility of polyaniline phase to silver ions, because during this procedure, the cryogels were again frozen and newly formed ice crystals might alter the existing macroporous structure. It was indeed observed that silver nitrate solution penetrated the aerogel, but the process was still relatively slow, and it took several days before the aerogel submerged. The silver

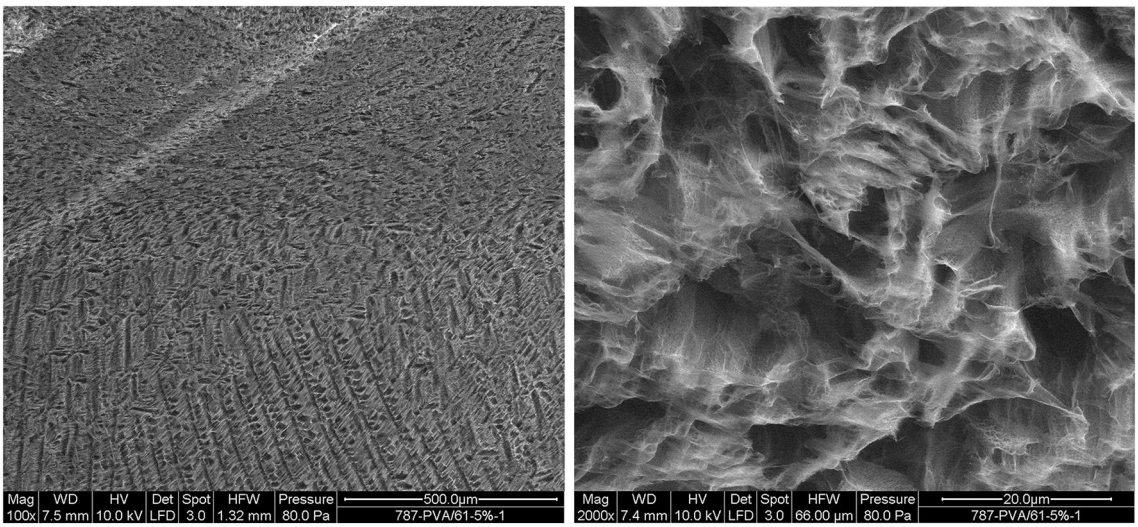

Fig. 3 Scanning electron micrographs of aerogel taken at lower (left) and higher magnifications (right)

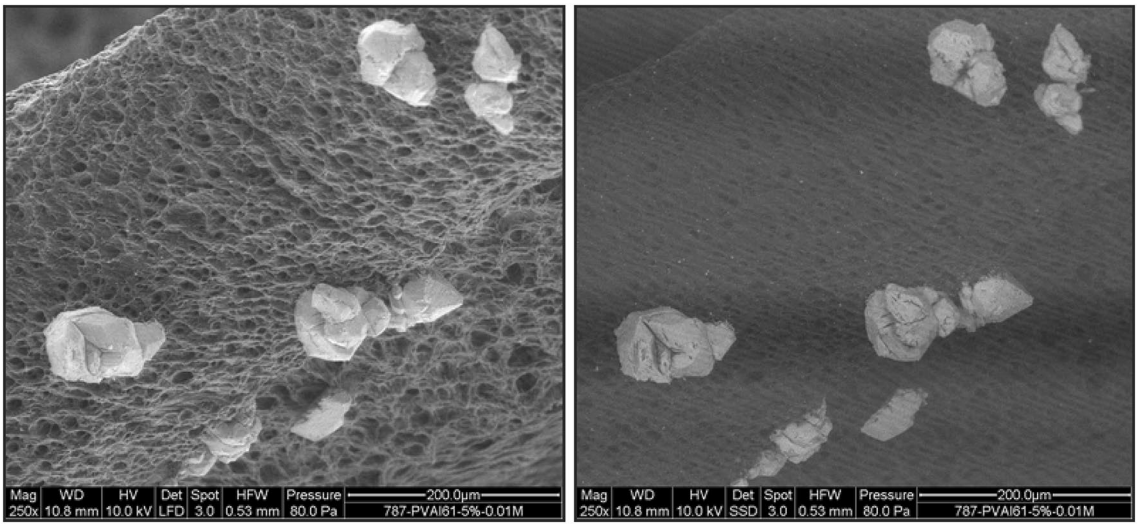

Fig. 4 Secondary electrons (left) and back-scattered electrons micrographs (right) of polyaniline/poly(vinyl alcohol) cryogels after reduction of 0.01 M silver nitrate

was obtained in relatively uniform microcubes of ca 1 µm edge (Figs. 5, 6). Much smaller silver nanocubes have often be produced during the reduction of silver ions, the typical edge size being ≈ 100 nm (Ashkarran et al. 2016; Zhou et al. 2016; Han et al. 2017b; Sarkar and Das 2017).

In the next series of experiments, the aerogel suspended in the silver nitrate solution was placed into

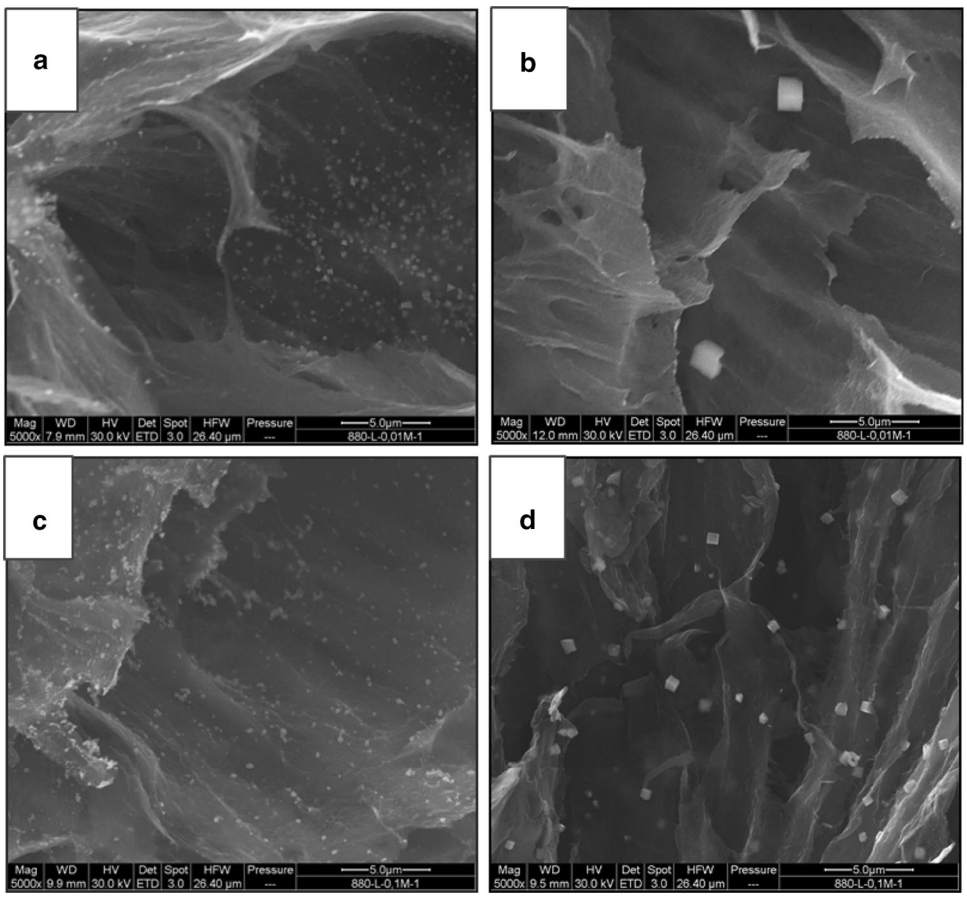

Fig. 5 Micrographs of polyaniline/poly(vinyl alcohol) aerogels after reduction of 0.01 M (**a**, **b**) and 0.1 M silver ions (**c**, **d**). Left column depicts the outer and right column the central part of the aerogel

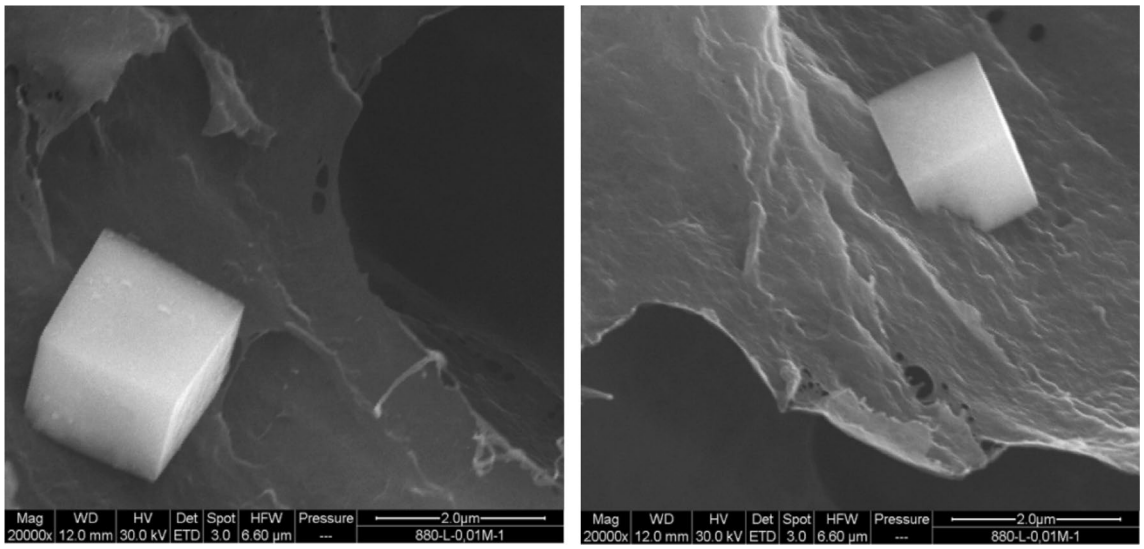

Fig. 6 Detailed views of silver cubes

rotational evaporator, and the pressure was reduced to release the air bubbles from the aerogel. Using this procedure, the aerogel was penetrated with the solution within ten of minutes. The results reported below nevertheless suggest that a fraction of pores was still not accessible to silver nitrate. The silver microcubes were also obtained in this case (Fig. 7).

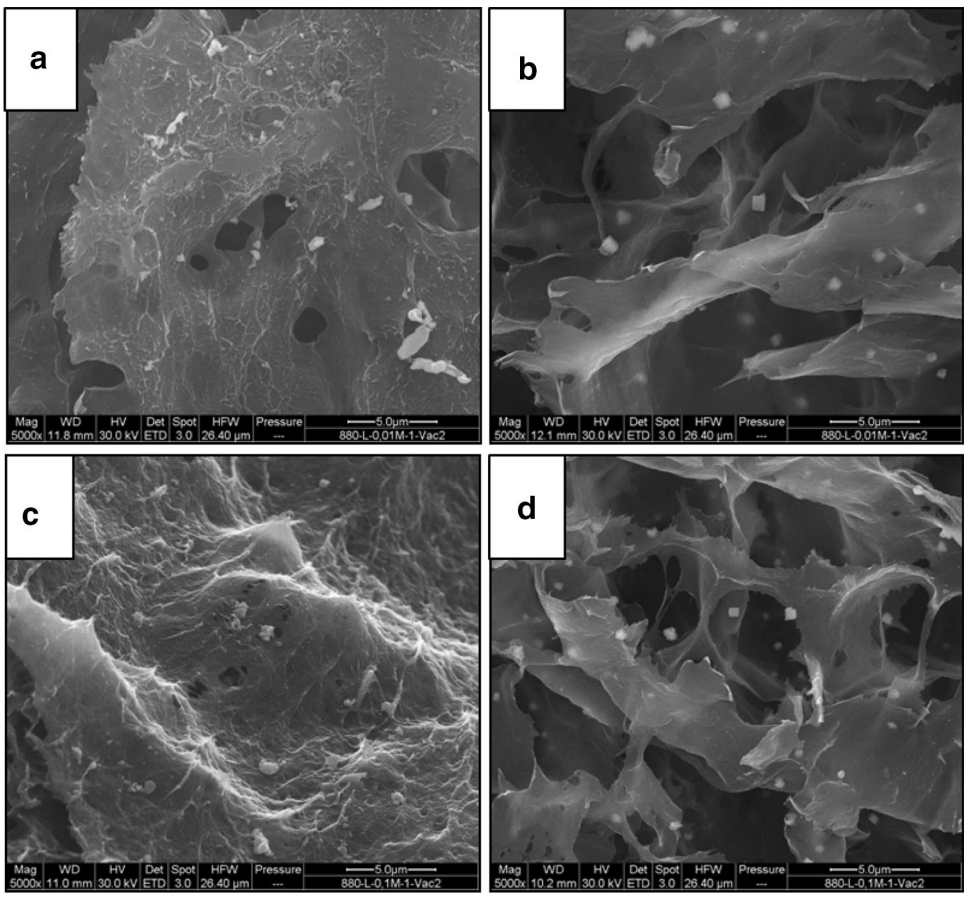

Fig. 7 Micrographs of vacuum-treated polyaniline/poly(vinyl alcohol) aerogels after reduction of 0.01 M (**a**, **b**) and 0.1 M silver ions (**c**, **d**). Left column depicts the outer and right column the central part of the aerogel

Silver content

Thermogravimetric analysis has been used for the determination of silver content as the residue (Fig. 8). It was observed for some aerogels that the mass started to increase above 670 °C, probably due to the oxidation of silver. It has to be stressed that the analysis must not be made in inert atmosphere when polyaniline would be carbonized (Trchová et al. 2009; Rozlívková et al. 2011a) and the residual mass would be considerably higher. The amounts used by this method are small, ≈ 10 mg, and it is often not possible to select a representative part in macroscopically non-uniform samples. For that reason, the silver contents display a significant scatter. The aerogels with deposited silver particles had improved thermal stability.

The composition of aerogels calculated from nitrogen content determined by elemental analysis revealed 58 wt% of polyaniline, the rest being poly(vinyl alcohol) matrix (Stejskal et al. 2017). By assuming the stoichiometry according to Fig. 1, 1 g of polyaniline should generate 0.6 g of silver. If all polyaniline in the aerogel were used in simple immersion for the reduction of silver ions, the resulting composite would contain 0.58 g polyaniline, 0.42 g poly(vinyl alcohol), and 0.35 g silver, i.e., the silver content would be 25.8 wt%.

The silver contents found in TGA amount to a few per cent for a simple immersion of aerogels into silver nitrate solutions (Table 1). In the case of vacuum-treated aerogels, the silver content was significantly higher, but still has not reached the expected value. The difference is explained by incomplete accessibility of polyaniline in micropores to the silver ions.

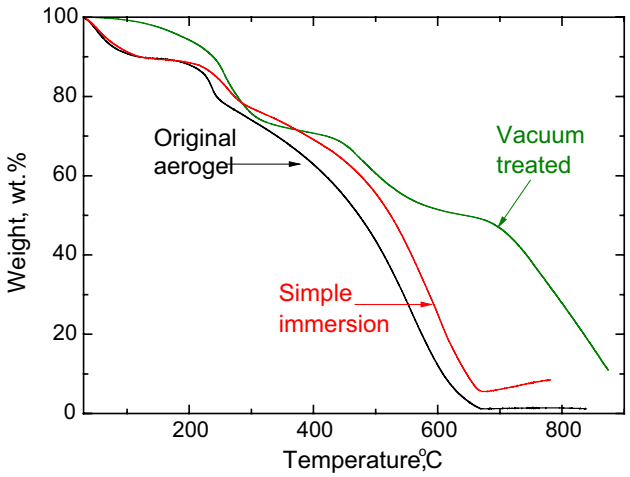

Fig. 8 Thermogravimetric analysis of original aerogel, and of freeze-dried aerogels that were simply immersed in 0.01 M silver nitrate solution or with prior vacuum treatment

Conductivity

Conductivity is important parameter of conducting polymers. In the case of aerogels, it is not easy to determine its true value, due to partial deprotonation of cryogels in water before freeze-drying; the presence of acid would be harmful to the freeze-drier. Both aerogel and vacuum-treated aerogel had different values of conductivity, which is connected to porosity type. The results indicate that the pores in vacuum-treated aerogels were more easily penetrated with water, the deprotonation process was more advanced, and the conductivity was reduced accordingly (Table 1). For that reason, to compare the conductivities of resulting aerogels with silver, the values have been normalized to silver-free aerogel. At low concentration of silver nitrate, the conductivity increased even two orders of magnitude for vacuum-treated aerogels (Table 1) due to silver generation. At higher concentration of silver nitrate, the decrease in conductivity was observed due to oxidation of conducting emeraldine form of polyaniline to non-conducting pernigraniline.

Raman spectra

The optical micrographs of aerogels containing silver display the bright and dark regions (Fig. 9). We suppose that bright regions are associated with polyaniline close to silver particles. Only the vacuum-treated series has further been characterized by Raman spectra recorded in bright and dark regions.

Raman spectra of polyaniline aerogels have been analyzed using a laser excitation line 514 nm at first (Fig. 10). It is known that Raman spectrum of polyaniline salt recorded

Table 1 Silver content determined by thermogravimetric analysis, the conductivity of pellets, σ, prepared by the compression of composites and its relative increase σ/σ_0 after exposure of aerogels to silver nitrate solutions with molar concentration, $[AgNO_3]$

$[AgNO_3]$, mol L^{-1}	Simple immersion			Vacuum treated		
	wt% Ag	σ (S cm^{-1})	σ/σ_0	wt% Ag	σ (S cm^{-1})	σ/σ_0
0	–	3.0×10^{-3}	1	–	2×10^{-5}	1
0.001	2.69	2.7×10^{-2}	9.0	13.4	2.6×10^{-3}	130
0.005	5.66	1.9×10^{-1}	63	11.0	2.8×10^{-3}	140
0.01	5.61	4.1×10^{-1}	140	10.9	2.7×10^{-3}	135
0.05	5.38	2.3×10^{-2}	7.7	11.6	1×10^{-5}	0.5
0.1	7.34	2.7×10^{-1}	90	4.38	3×10^{-8}	0.001

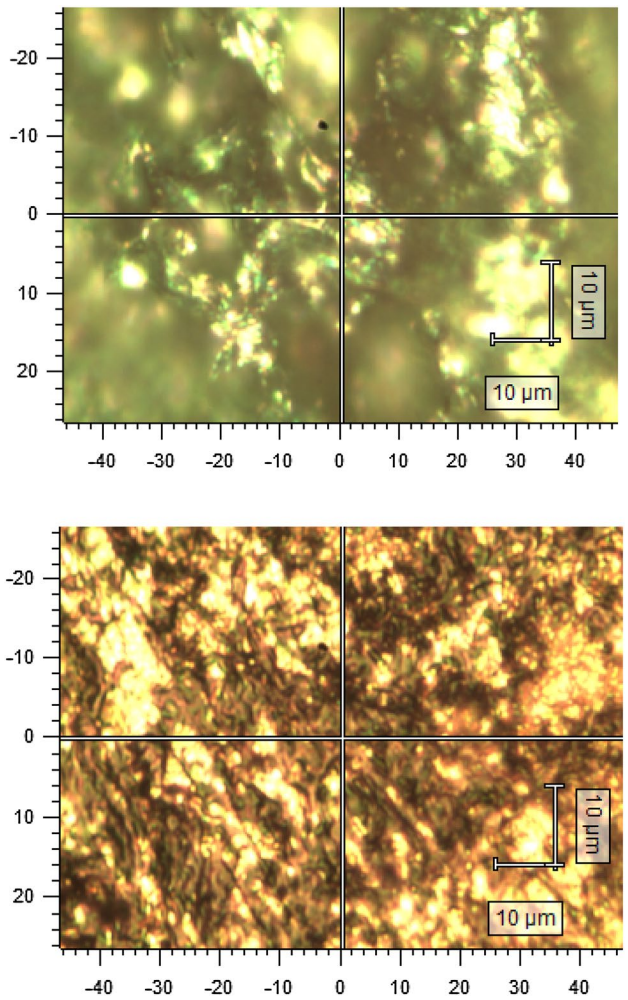

Fig. 9 Optical micrographs of polyaniline/poly(vinyl alcohol) aerogel prepared by immersion in 0.001 M silver nitrate and drying before (top) and after compression into a pellet (bottom)

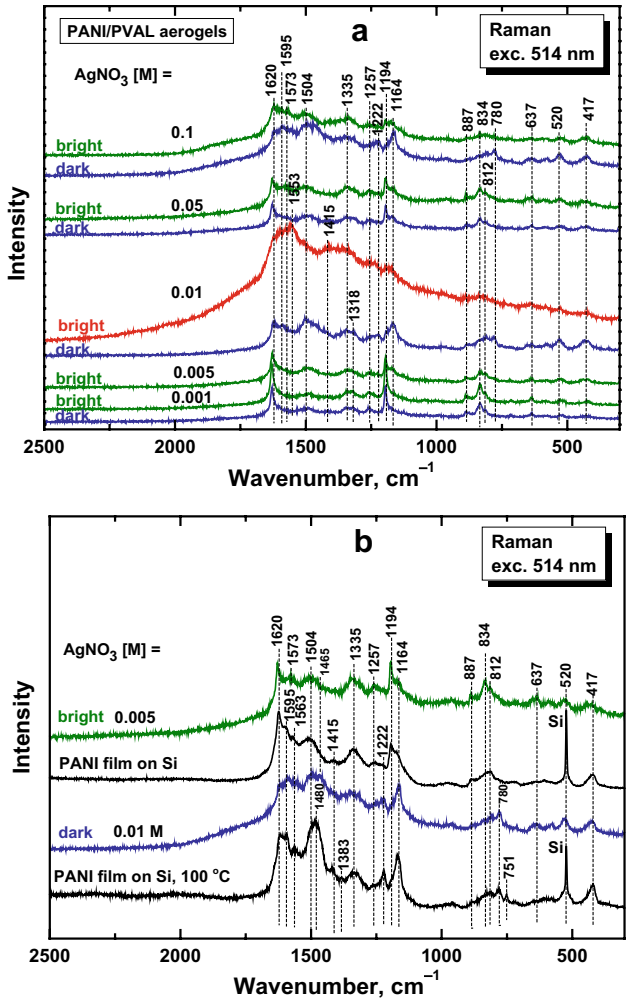

Fig. 10 **a** Raman spectra of polyaniline aerogels immersed in solution of silver nitrate of various molar concentrations, [$AgNO_3$]. Spectra were recorded in bright and dark regions of samples. **b** Comparison of Raman spectra of samples immersed in solution of 0.005 and 0.001 M silver nitrate in bright and dark regions with the spectra of polyaniline standard films (Stejskal and Sapurina 2005) deposited in situ on silicon support at ambient temperature and after heating at 100 °C. Laser excitation line was 514 nm

at this excitation line is in resonance with the "reduced" units (with the energy of transitions in benzenoid units). Raman spectra taken at bright regions differ from the spectra corresponding to dark regions (Fig. 10a). The former are close to the spectra of the standard polyaniline film (Stejskal and Sapurina 2005) deposited in situ on silicon (Fig. 10b). The most pronounced band at 1620 cm^{-1} corresponds to the C–C-stretching vibrations of the benzene ring. We observed other bands typical of polyaniline salt films which have previously been described (Rozlívková et al. 2011b; Morávková et al. 2012; Trchová et al. 2014). In some cases, they are strongly enhanced due to the resonance effect on silver particles, which may cause the burning of sample (the spectrum for 0.01 M silver nitrate in Fig. 10a).

The Raman spectra at dark regions taken with a 514 nm laser resemble the Raman spectrum of standard polyaniline film heated to 100 °C (Fig. 10b). The spectra were transformed to that of the deprotonated form of polyaniline (Morávková et al. 2012). Especially, the peak situated at 1620 cm^{-1} was reduced to a shoulder of the band with maximum at 1595 cm^{-1}, which corresponds to the C=C-stretching vibrations of the quinonoid rings. The broad band of C=N-stretching vibrations in quinonoid units observed at 1480 cm^{-1} is present in the spectra (Fig. 10). We conclude that the samples are deprotonated after washing in water in dark regions. The transformation into pernigraniline form of polyaniline cannot be excluded.

Polyaniline aerogels compressed into pellets for conductivity measurements were analyzed with a laser excitation line 785 nm (Fig. 11). Using this excitation wavelength, various semiquinone cation-radical structures

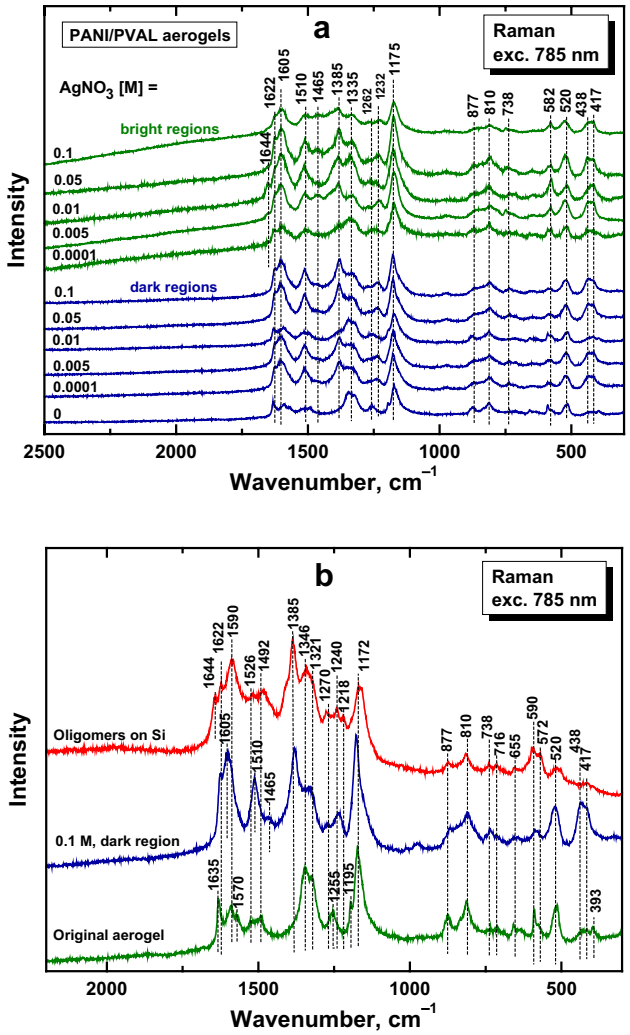

Fig. 11 **a** Raman spectra of polyaniline/poly(vinyl alcohol) aerogels after immersion in solutions of silver nitrate of various concentrations, freeze-drying, and pressing into pellets. Spectra were recorded in bright and dark regions of samples. **b** Comparison of Raman spectra of samples before and after immersion in solution of 0.1 M silver nitrate and recorded in dark region with the spectrum of the first product of aniline oxidation deposited on silicon. Laser excitation line was 785 nm

assigned to the C~N$^{+\bullet}$ vibrations of polaronic sites should be in resonance with the energy of incident radiation. We have previously demonstrated that before immersion in silver nitrate solution, the Raman spectra of polyaniline aerogels were also for this laser excitation line very close to the Raman spectrum of standard polyaniline film (Morávková et al. 2012; Trchová et al. 2014; Stejskal et al. 2017). We conclude that polyaniline was generated on the surface of poly(vinyl alcohol) skeleton during aniline oxidation, and as a consequence, its molecular structure is close to the molecular structure of thin polyaniline films. The contribution of supporting poly(vinyl alcohol) to the surface-sensitive Raman spectra has not been observed (Stejskal et al. 2017).

In the Raman spectrum of original aerogel taken before immersion in silver nitrate and pressed into pellet (Fig. 11b), we find a sharp peak at 1635 cm^{-1} (connected with the formation of crosslinked units with phenazine-like structure or benzoquinonediimine mixed with C–C-stretching vibrations of the benzenoid ring), the band at 1590 cm^{-1} (C=C-stretching vibrations in the oxidized quinonoid units), with a shoulder at 1570 cm^{-1} (C–C vibration in the quinonoid ring of pernigraniline and pseudomauveine base-like units), the broad band with maxima at 1526 and 1492 cm^{-1} (the last is associated with the C=N-stretching vibrations in quinonoid units). The band at 1346 cm^{-1} is attributed to the C~N$^{+\bullet}$ vibrations of delocalized polarons. Benzene- and quinone-ring-deformation vibrations are associated with the band at 1255 cm^{-1}. The strong peak at 1172 cm^{-1} corresponds to the C–H-bending vibrations of the semi-quinonoid ring. It has a shoulder located at 1195 cm^{-1}. In the low-wavenumber region, we observe the bands with local maxima at 877, 810, 738, 716, 655, 590, 520, 438, 417, and 393 cm^{-1} that correspond to the various ring-deformation vibrations and crosslinked oligomeric structures observed with this excitation. The spectrum slightly differs from the spectrum of thin polyaniline films deposited on silicon (Morávková et al. 2012; Trchová et al. 2014) after pressing of aerogel into a pellet.

Raman spectra of aerogels after immersion in silver nitrate solutions and pressed into pellet dramatically changed (Fig. 11a). A typical spectrum taken in the dark region of the sample immersed in 0.1 M silver nitrate is compared with the spectrum of sample before immersion, is shown in Fig. 11b. The peak at 1635 cm^{-1} disappeared. The band observed earlier at 1590 cm^{-1} shifted to 1605 cm^{-1} and a shoulder at 1622 cm^{-1} appeared in the spectrum. Two maxima situated at 1526 and 1492 cm^{-1} merged into a new strong band with a maximum at 1510 cm^{-1}. A new strong band at 1385 cm^{-1} with a shoulder at about 1335 cm^{-1} appeared in the spectrum. The former has also been detected in the spectra of oligomeric products, isolated after first exothermic phase of the oxidation of aniline (Morávková et al. 2012) (oligomers in Fig. 11b), where it has been assigned to the C~N$^{+\bullet}$ vibrations of more oxidized and localized polarons band. The bands at 1220 and 1175 cm^{-1} of C–N and C–H vibrations of quinonoid structure are found in the spectrum. The bands in the low-wavenumber region have slightly changed after immersion in the solution of silver nitrate. The observed Raman spectrum also exhibits some features of the Raman spectrum of *N*,*N*'-diphenyl-1,4-phenylenediamine (Quillard et al. 1994; Boyer et al. 1997).

Conclusions

Polyaniline-based cryogels represent a novel type of soft macroporous conducting materials. The immersion of swollen polyaniline/poly(vinyl alcohol) cryogels into aqueous solutions of silver nitrate led only to the limited reduction of silver ions to silver at the cryogel surface. This is due to the closed macropores and restricted penetration of silver ions to gel interior.

The immersion of freeze-dried cryogels, i.e., aerogels, into silver nitrate solution led to more efficient generation of silver in a form of microcubes due to the partial opening of pores. The silver content still increased when the penetration of silver nitrate solution was enhanced by vacuum treatment. The maximum silver content was 13 wt%, i.e., about one half of the stoichiometric expectation.

The conductivity assessment was complicated by the deprotonation phenomena in polyaniline associated with the cryogel processing. As the concentration of silver nitrate increased, the conductivity also increased due to the produced silver at first. Later, the oxidation of conducting emeraldine form to non-conducting pernigraniline predominated, and the conductivity decreased again. Raman spectra revealed the heterogeneous structure of the composite material.

Acknowledgements The financial support of the Czech Science Foundation (16-02787S) is gratefully acknowledged.

References

Ashkarran AA, Daemi S, Derakhshi M (2016) Destructive effect of solar light on morphology of colloidal silver nanocubes. Colloid J 78:577–585. https://doi.org/10.1134/S1061933X16050021

Bober P, Stejskal J, Trchová M, Prokeš J (2011) The preparation of conducting polyaniline–silver and poly(*p*-phenylenediamine)–silver nanocomposites in liquid and frozen reaction mixtures. J Solid State Electrochem 15:2361–2368. https://doi.org/10.1007/s10008-011-1414-8

Bober P, Stejskal J, Trchová M, Prokeš J (2014) In-situ prepared polyaniline-silver composites: single- and two-step strategies. Electrochim Acta 122:259–266. https://doi.org/10.1016/j.electacta.2013.10.001

Boyer M, Quillard S, Louarn G, Lefrant S, Rebourt E, Monkman AP (1997) Oxidized model compounds of polyaniline studied by resonance Raman spectroscopy. Synth Met 84:787–788. https://doi.org/10.1016/S0379-6779(96)04146-X

Guiseppi-Elie A (2010) Electroconductive hydrogels: synthesis, characterization and biomedical applications. Biomaterials 31:2701–2716. https://doi.org/10.1016/j.biomaterials.2009.12.052

Han J, Wang MG, Hu YM, Zhou CQ, Guo R (2017a) Conducting polymer-noble metal nanoparticle hybrids: synthesis mechanism application. Prog Polym Sci 70:52–91. https://doi.org/10.1016/j.progpolymsci.2017.04.002

Han HJ, Yu T, Kim WS, Im SH (2017b) Highly reproducible polyol synthesis for silver nanocubes. J Cryst Growth 469:48–53. https://doi.org/10.1016/j.jcrysgro.2016.09.038

Hou YH, Feng JT, Wang YC, Li LC (2016) Enhanced antimicrobial activity of Ag-doped ZnO/polyaniline nanocomposites. J Mater Sci: Mater Electron 27:6615–6622. https://doi.org/10.1007/s10854-016-4669-0

Khan A, Asiri AM, Khan AAP, Sirajuddin, Gupta V, Inamuddin (2016) Room temperature preparation, electrical conductivity, and thermal behaviour evaluation on silver nanoparticle embedded polyaniline tungstophosphate nanocomposite. Polym Compos 37:2460–2466. https://doi.org/10.1002/pc.23433

Konyushenko EN, Stejskal J, Trchová M, Blinova NV, Holler P (2008) Polymerization of aniline in ice. Synth Met 158:927–933. https://doi.org/10.1016/j.synthmet.2008.06.015

Lozinsky VI, Okay O (2014) Basic principles of cryotropic gelation. Adv Polym Sci 263:49–101. https://doi.org/10.1007/978-3-319-05846-7_2

Ma HY, Yan SQ, Pu XP, Shao X, Li YW, Gong J, Deng YL (2016) Freezing-mediated polymerization of Ag nanoparticle-embedded polyaniline belts with polyoxymetalate as doping acid exhibiting UV-photosensitivity. RSC Adv 6:46475–46478. https://doi.org/10.1039/c6ra06216d

Maráková N, Humpolíček P, Kašpárková V, Capáková Z, Martinková L, Bober P, Trchová M, Stejskal J (2017) Antimicrobial activity and cytotoxicity of cotton fabric coated with conducting polymers, polyaniline or polypyrrole, and with deposited silver nanoparticles. Appl Surf Sci 396:169–176. https://doi.org/10.1016/j.apsusc.2016.11.024

Morávková Z, Trchová M, Exnerová M, Stejskal J (2012) The carbonization of thin polyaniline films. Thin Solid Films 520:6088–6094. https://doi.org/10.1016/j.tsf.2012.05.067

Pan C, Lv YH, Gong HM, Jiang QK, Miao S, Liu JY (2016) Synthesis of Ag/PANI@MnO_2 core–shell nanowires and their capacitance behavior. RSC Adv 6:17415–17422

Pande NS, Jaspal D, Ambekar J (2017) Poly(*N*-ethyl aniline)/Ag nanocomposite as humidity sensor. Int J Nanosci 16:1650037. https://doi.org/10.1142/S0219581X1650037X

Pandey AK, Pandey PC, Agarwal NR, Das I (2017) Synthesis and characterization of dendritic polypyrrole silver nanocomposite and its application as a new urea biosensor. J Appl Polym Sci 135:45705. https://doi.org/10.1002/app.45705

Quillard S, Louarn G, Lefrant S (1994) Vibrational analysis of polyaniline: a comparative study of leucoemeraldine, emeraldine, and pernigraniline bases. Phys Rev B 50:12496–12508 **(WOS: A1994PR26100024)**

Rahman MM, Khan A, Marwani HM, Asiri AM (2016) Hydrazine sensor based on silver nanoparticle-decorated polyaniline tungstophosphate nanocomposite for use in environmental remediation. Microchim Acta 18:1787–1796. https://doi.org/10.1007/s00604-016-1809-4

Rozlívková Z, Trchová M, Exnerová M, Stejskal J (2011a) The carbonization of granular polyaniline to nitrogen-containing carbon. Synth Met 161:1122–1129. https://doi.org/10.1016/j.synthmet.2011.03.034

Rozlívková Z, Trchová M, Šeděnková I, Špírková M, Stejskal J (2011b) Structure and stability of thin polyaniline films deposited in situ on silicon and gold during precipitation and dispersion polymerization of aniline hydrochloride. Thin Solid Films 519:5933–5941. https://doi.org/10.1016/j.tsf.2011.03.025

Salam MA, Obaid AY, El-Shishtawy RM, Mohamed SA (2017) Synthesis of nanocomposites of polypyrrole/carbon nanotubes/silver nano particles and their application in water disinfection. RSC Adv 7:16878–16884. https://doi.org/10.1039/c7ra01033h

Saleh HH, Ali Zi, Afify TA (2016) Synthesis of Ag/PANI core shell nanocomposites using ionizing radiation. Adv Polym Technol 35:335–344. https://doi.org/10.1002/adv.21560

Sarkar S, Das R (2017) PVP capped silver nanocubes assisted removal of glyphosate from water—a photoluminescence study. J Hazard Mater 339:54–62. https://doi.org/10.1016/j.jhazmat.2017.06.014

Stejskal J (2013) Conducting polymer-silver composites. Chem Pap 67:814–848. https://doi.org/10.2478/s11696-012-0304-6

Stejskal J (2017) Conducting polymer hydrogels. Chem Pap 71:269–291. https://doi.org/10.1007/s11696-016-0072-9

Stejskal J, Sapurina I (2005) Polyaniline: thin films and colloidal dispersions. Pure Appl Chem 77:815–826. https://doi.org/10.1351/pac200577050815

Stejskal J, Kratochvíl P, Helmstedt M (1996) Polyaniline dispersions.5. Poly(vinyl alcohol) and poly(N-vinylpyrrolidone) as steric stabilizers. Langmuir 12:3389–3392. https://doi.org/10.1021/la9506483

Stejskal J, Sapurina I, Trchová M (2010) Polyaniline nanostructures and the role of aniline oligomers in their formation. Prog Polym Sci 35:1420–1881. https://doi.org/10.1016/j.progpolymsci.2010.07.006

Stejskal J, Bober P, Trchová M, Kovalcik A, Hodan J, Hromádková J, Prokeš J (2017) Polyaniline cryogels supported with poly(vinyl alcohol): soft and conducting. Macromolecules 50:972–978. https://doi.org/10.1021/acs.macromol.6b02526

Tang L, Duan F, Chen MQ (2016) Silver nanoparticle decorated polyaniline/multiwalled super-short carbon nanotube nanocomposites for supercapacitor applications. RSC Adv 6:65012–65019. https://doi.org/10.1039/c6ra12442a

Trchová M, Stejskal J (2010) The reduction of silver nitrate to metallic silver inside polyaniline nanotubes and on oligoaniline microspheres. Synth Met 160:1479–1486. https://doi.org/10.1016/j.synthmet.2010.05.007

Trchová M, Konyushenko EN, Stejskal J, Kovářová J, Ćirić-Marjanović G (2009) The conversion of polyaniline nanotubes to nitrogen-containing carbon nanotubes and their comparison with multiwalled carbon nanotubes. Polym Degrad Stab 94:912–938. https://doi.org/10.1016/j.polymdegradstab.2009.03.001

Trchová M, Morávková Z, Bláha M, Stejskal J (2014) Raman spectroscopy of polyaniline and oligoaniline thin films. Electrochim Acta 122:28–38. https://doi.org/10.1016/j.electacta.2013.10.133

ul Haque S, Inamuddin, Nasar A, Rajender B, Khan A, Asiri AM, Ashraf GM (2017) Optimization of glucose powered biofuel cell anode developed by polyaniline–silver as electron transfer enhancer and ferritin as biocompatible redox mediator. Sci Rep 7:12703. https://doi.org/10.1038/s41598-017-12708-6

Wang YF, Shen YH, Xie AJ, Chen SH (2013) One-step synthesis of Ag@PANI nanocomposites and their application to detection of mercury. Mater Chem Phys 140:487–492. https://doi.org/10.1016/j.matchemphys.2013.03.058

Wang YL, Bian L, Tan DX, Chen S, Gan Y (2017a) Sonochemical synthesis of "sea-island" structure silver/polyaniline nanocomposites for the detection of L-tyrosine. J Thermoplastic Compos Mater 30:1033–1044. https://doi.org/10.1177/0892705715614387

Wang XF, Feng SJ, Zhao W, Zhao DL, Chen SH (2017b) Ag/polyaniline heterostructured nanosheets loaded with g-C3N4 nanoparticles for highly efficient photocatalytic hydrogen generation under visible light. New J Chem 41:9354–9360. https://doi.org/10.1039/c7nj01903c

Wang HH, Wen H, Hu B, Fei CQ, Shen YD, Sun LY, Yang D (2017c) Facile approach to fabricate waterborne polyaniline nanocomposites with environmental benignity and high physical properties. Sci Rep 7:43694. https://doi.org/10.1038/srep43694

Xu FG, Xie S, Xu H, Chen X, Yu H, Wang L (2017) Interlaced silver nanosheets grown on polyaniline coated carbon foam as efficient three dimensional surface enhanced Raman scattering substrate for molecule sensing. Appl Surf Sci 410:566–573. https://doi.org/10.1016/j.apsusc.2017.03.174

Yi Q, Chu H, Tang M, Zhang Y, Liu X, Zhou Z, Nie H (2014) A novel membraneless direct hydrazine/air fuel cell. Fuel Cells 14:827–833. https://doi.org/10.1002/fuce.201400098

Zhang J, Guan PP, Li W, Shi ZQ, Zhai H (2016) Synthesis and characterization of a polyaniline/silver nanocomposite for the determination of formaldehyde. Instrum Sci Technol 44:249–258. https://doi.org/10.1080/10739149.2015.1104507

Zhao S, Huang LC, Tong TZ, Zhang W, Wang Z, Wang JX, Wang SC (2017) Antifouling and antibacterial behaviour of polyethersulfone membrane incorporating polyaniline@silver nanocomposite. Environ Sci Water Res Technol 3:710–719. https://doi.org/10.1039/c6ew00332

Zhou S, Li JH, Gilroy KD, Tao J, Zhu CL, Yang X, Sun XJ, Xia YN (2016) Facile synthesis of silver nanocubes with sharp corners and edges in an aqueous solution. ACS Nano 10:9861–9870. https://doi.org/10.1021/acsnano.6b05776